Augmentation of Heat Transfer Through Heat Exchanger With and Without Fins by Using Nano fluids

Dr. Khalid Faisal Sultan
Lecture
Electromechanical. Eng. Dept
University of Technology

Abstract

This study was carried out to study the effect of silver and oxide zirconium – oil nanofluids on enhancement heat transfer in a heat exchanger with and without fins by changing flow direction. This study was done by changing the parallel flow configuration into counter flow configuration under laminar flow regime. The properties of nanofluids (density, viscosity, thermal conductivity and specific heat) are practically measured. The two types of nanofluids at 1%, 2%, 3%, 4% and 5% particle volume concentration were prepared by two step method. The nanofluid was applied in a heat exchanger with and without fins to enhance heat transfer. The measured results show that silver with oil nanofluid gives maximum heat transfer enhancement compared with oxide zirconium nanofluid used. The presence of Ag and ZrO_2 nanoparticles attributes to the generation of strong nanoconvection current and better mixing. The effect of different parameters such as flow Reynolds number, nanofluid temperature, concentration and type of nanoparticle on heat transfer coefficient and pressure drop of the flow are studied. The obtained results show an increase in heat transfer coefficient to (Ag + oil) and (ZrO_2 + oil) for heat exchanger with fins 38.5 % ,25.33% while without fins 22.41% and 16.25% respectively at concentration of 5%vol compared with base fluid (oil). The heat transfer coefficient and pressure drop is increased by using nanofluids (Ag + oil, ZrO_2 + oil) instead of the base fluid (oil). The shear stress of nanofluids increases with an increase in concentration of nanoparticles for both parallel flow and counter flow. No much The precent work . impact of changing flow direction on overall heat transfer coefficient decided that the nanofluids behaviors are close to the typical Newtonian fluids through the relationship between viscosity and shear rate for ranging from (1% vol – 5% vol). This article indicated that the thermal performance from nanofluids that contain metal nanoparticles show more enhancements compared to oxide nanofluids due to higher thermal conductivity for the silver. Moreover to performance index are used to present the corresponding flow and heat transfer technique.

***Keywords*:** Nanofluids, Heat exchanger with and without fins, Overall heat transfer coefficient, Performance index.

تحسين انتقال الحرارةِ خلال مبادل حراري مع وبدون زعانف باستعمال المواد النانوية

د. خالد فيصل سلطان
مدرس
قسم الهندسة الكهرو ميكانيكية
الجامعة التكنولوجية

الخلاصة

تقدّمُ هذه المقالةِ دراسةً تجريبيةً عن تأثير الموائع الفائقة الدقة مثل (الفضة مع الزيت، وأوكسيد الزركونيوم مع الزيت) على تحسينِ نقلِ الحرارةِ والجريان في مبادل حراري بدون ومع وجود زعانف وبتغير اتجاه الجريان . هذه الدراسة تمت بتغير اتجاه الجريان من جريان متوازي الى جريان متعاكس تحت شرط جريان طباقي . كما وتم قياس الخواص الحرارية للموائع النانوية (الكثافة ،الموصلية الحرارية ،الحرارة النوعية، اللزوجة) عملياً. أثنان مِنْ أنواع الجزئيات النانوية استعملت في هذه الدراسة وهي الفضة (Ag (40nm)) وأكسيد الزركونيوم (ZrO_2 (60nm)) بالإضافة إلى مائع الأساس (زيت) وبتراكيز تَتراوحُ مِنْ (1 – 5 %) وقد تم تحضير هذه الموائع بطريقة الخطوتين. المائع النانوي يمكن ان يطبق في مبادل حراري مع وجود او عدم وجود الزعانف في تحسين انتقال الحرارة . النتائج بينت ان استخدام المائع النانوي من الفضة والزيت يعطي اقصى تحسين من اوكسيد الزركونيوم والزيت . ان وجود هذه الجزئيات النانوية مثل الفضة واوكسيد الزركونيوم يؤدي الى توليد تيارات حمل نانوية وبالتالي يحصل خلط جيد . أنّ تأثيرَ العوامل المختلفةِ مثل عدد رينولدز للجريان ، درجة حرارة المائع النانوية ونوع وتركيز الجزئيات النانوية على معاملِ انتقالِ الحرارةِ وهبوطِ ضغطِ الجريان قد تم دراسته. كما بينت الدراسة نسب التحسين في معامل نقل الحرارة باستخدام الفضة والزيت ،واوكسيد الزركونيوم والزيت في مبادل حراري مع وجود او عدم وجود الزعانف % 38.5, 25.33% ,22.41% , 16.25% على الترتيب وعند تركيز 5% vol بمقارنة مع الزيت كما بينت الدراسة ان معامل انتقال الحرارة وانحدار الضغط يزداد عند استخدام المائع النانوي بدل من الزيت . كما اوضحت الدراسة ان اجهاد القص للمائع النانوي يزداد مع زيادة التركيز للجريان المتوازي والمتعاكس وقد بينت النتائج انه لا تأثير كبير على تغير اتجاه الجريان على معامل انتقال الحرارة الكلي . هذه المقالة اقرت ان الموائع النانوية هي موائع نيوتينية من خلال علاقة اللزوجة واجهاد القص والى مدى (1 – 5 %) بالاضافة الى انها بينت ان الاداء الحراري للموائع النانوية التي تحتوي جزئيات نانوية معدنية اكثر تحسين بالمقارنة مع جزئيات نانوية تحتوي أوكسيد الزركونيوم بسب الموصلية الحرارية العالية للفضة . علاوة على ذلك تم استخدام عامل الاداء لتقيم التدفق وانتقال الحرارة.

1. Introduction

Thermal load removal is a great concern in many industries including power plants, production and chemical processes, transportation and electronics. In order to meet the ever increasing need for cooling the high heat flux surfaces, different enhanced heat transfer techniques have been suggested. Most of these methods are based on structure variation, vibration of heated surface, injection or suction of fluid and applying electrical or magnetic fields which are well documented in literature A.E. Bergles [1973] and J.R. Thome [2006]. However, applying these enhanced heat transfer techniques is no longer feasible for cooling requirement of future generation of microelectronic systems, since they would result in undesirable cooling system size and low efficiency of heat exchangers. To obviate this problem, nanofluids with enhanced thermo-fluidic properties have been proposed since the past decade. Nanofluid is a uniform dispersion of nanometer sized particles inside a liquid which was first pioneered by Choi [2008]. Excellent characteristics of nanofluids such as enhanced thermal conductivity, long time stability and little penalty in pressure drop increasing and tube wall abrasion have motivated many researchers to study on thermal and flow behavior of nanofluids. These studies are mainly focused on effective thermal conductivity, phase change behavior, tribological properties, flow and convective heat transfer of nanofluids. A wide range of experimental and theoretical studies has been performed on effective thermal conductivity of nanofluids within past decade. In these studies, the effect of different parameters such as particle concentration, particle size, mixture temperature and Brownian motion on thermal conductivity of nanofluids was investigated. The results showed

an increase in thermal conductivity of nanofluid with the increase of nanoparticles concentration and mixture temperature M. Chandrasekar et al. [2010], W. Yu et al., [2010], H.A. Mintsa et al. [2009], R.S. Vajjha et al.[2009]. Also it was shown that larger enhancement in thermal conductivity is attributed to the finer particle size H.A. Mintsa et al. [2009], R.S. Vajjha et al.[2009], N.R. Karthikeyan et al.[2008]. Due to the enhanced thermal properties of nanofluids, majority of recent studies are focused on convective heat transfer behavior of nanofluids in laminar and turbulent flows. Almost all of these works report the enhancement of nanofluid convective heat transfer. Several numerical and experimental studies have considered nanofluid convective heat transfer in turbulent flow S.M. Fotukian et al.[2010], S.M. Fotukian et al.[1998], W.C. Williams et al. [2008], Y. He et al.[2007]. Some other studies have investigated the convective heat transfer of nanofluids in laminar flow.

Wen and Ding [2004] have studied Al_2O_3/water nanofluid heat transfer in laminar flow under constant wall heat flux and reported an increase in nanofluid heat transfer coefficient with the increase in Reynolds number and nanoparticles concentration particularly at the entrance region. Convective heat transfer of CNT nanofluids in laminar regime with a constant heat flux wall boundary condition was investigated by Ding et al. [2006]. They observed a maximum enhancement of 350% in convective heat transfer coefficient of 0.5 wt.% CNT/water nanofluid at Re=800. In addition, a few works have studied friction factor characteristics of nanofluids flow besides the convective heat transfer. Xuan and Li [2003] investigated the flow and convective heat transfer characteristics for Cu/water nanofluids inside a straight tube with a constant heat flux at the wall, experimentally. Results showed that nanofluids give substantial enhancement of heat transfer rate compared to pure water. They also claimed that the friction factor for the nanofluids at low volume fraction did not produce extra penalty in pumping power. In laminar flow, Chandrasekar et al. [2010] investigated the fully developed flow convective heat transfer and friction factor characteristics of Al_2O_3/water nanofluid flowing through a uniformly heated horizontal tube with and without wire coil inserts. They concluded that for the nanofluid with a volume concentration of 0.1%, the Nusselt number increased up to 12.24% compared to that of distilled water. However, the friction factors of the same nanofluid were almost equal to those of water under the same Reynolds numbers. Another technique which is employed for heat transfer augmentation is using helical tubes instead of straight tubes. Due to their compact structure and high heat transfer coefficient, helical tubes have been introduced as one of the passive heat transfer enhancement techniques and are widely used in various industrial applications such as heat recovery processes, air conditioning and refrigeration systems, chemical reactors, food and dairy processes. Single-phase heat transfer characteristics in the helical tubes have been widely studied by researchers both experimentally and theoretically. The heat transfer rates between a helically coiled heat exchanger and a straight tube heat exchanger were compared by Prabhanjan et al. [2002]. Results showed that the geometry of the heat exchanger and the temperature of the water bath surrounding the heat exchanger affected the heat transfer coefficient.

Xin et al. [1997] studied the effects of coil geometries and the flow rates of air and water on pressure drop in both annular vertical and horizontal helical pipes. The test sections with three different diameters of inner and outer tubes were tested. The results showed that the transition from laminar to turbulent flow covers a wide Reynolds number range. On the basis

of the experimental data, a correlation of the friction factor was developed. The maximum deviation of the friction factor from experiments and the correlation was found to be 15%. Choi and colleagues [2008] used spherical and rod shape Al_20_3 and spherical AIN nanoparticles dispersed in transformer oil to make nanofluids. All three types of nanofluids showed a small enhancement in the heat transfer coefficient at a Reynolds number range of 100 to 500. A maximum of 20% increase was observed for the AIN/transformer oil based nanoparticles at a volume fraction of 0.5%. Thorough literature survey showed that comparatively little work focused on experimental study in helical finned tube and shell heat exchanger.

In the present study, the main purpose of this work is to study and explore the enhancement in heat transfer characteristics and its effect on pressure drop of various concentrations of two types of nanofluids in a heat exchanger with and without fins and by changing the flow directions. As well as the effect study of oil as the base fluid

2. Nanofluid preparation

The studied nanofluid is formed by silver (Ag (40 nm)) and oxide zirconium (ZrO_2) (60 nm) nanoparticles and the two – step method was used to prepare nanofluids. Nanofluid samples were prepared by dispersing pre – weighed quantities of dry particles in base fluid (oil). In a typical procedure, the pH of each nanofluids mixture was measured .The mixtures were then subjected to ultrasonic mixing [100 kHz, 300 W at 25 – 30 C^0, Toshiba, England] for one hour to break up any particle aggregates. The acidic pH is much less than the isoelectric point [iep] of these particles, thus ensuring positive surface charges on the particles. The surface enhanced repulsion between the particles, which resulted in uniform dispersions for the duration of the experiments. An image nanofluids containing (Ag (40 nm)) and oxide zirconium (ZrO_2) (60 nm) is display in figure (1). Nanofluids with different volume fractions (Φ = 1, 2, 3,4 and 5vol %)are used. The nanofluid of this study was included 20W50 engine oil (Castrol Company) (GTX) and nanoparticles (US Research Nano materials, Inc). Their properties are shown in table 1, 2 and 3 respectively.

Fig.1 Show nanofluids for Ag+ oil, ZrO_2+oil and oil

Table1: The properties of engine oil, US Research Nanomaterials [2014]

Name	SAE 20W50
Density at 15.6°C (kg/m^3)	893
Viscosity at 100°C (cSt)	17
Viscosity index	115
Total alkalinity (mgKOH/g)	6
Minimum ignition point	214
Minimum Pour point (°C)	– 24

Table2: The properties of Nano powder Ag [2014]

Silver Nano powder Ag, 99%, 40 nm	
Purity	>99%
crystal phases	Monoclinic
APS	40 nm
SSA	– 40 m^2/g 20
Color	Lead
Morphology	Nearly spherical
True density	10.500 g/cm^3

Table3: The properties of Nano powder ZrO_2 [2014]

Zirconium oxide Nano powder ZrO_2, 99%, 60 nm	
Purity	>99%
crystal phases	Monoclinic
APS	60 nm
SSA	– 40 m^2/g 20
Color	white
Morphology	spherical
True density	5.890 g /cm^3

3. Experimental setup

The experimental set up is designed for two experimental. The experimental loop was designed for convective heat transfer and friction factor. The first experimental set up consist of heat exchanger without fins on the internal tube is made of Pyrex glass external tube (OD) of 180 mm, copper internal tube (ID) of 40 mm without finned and length 1200mm. The set – up has tube side loop and shell side loop. The tube side loop handles two types of nanofluids used silver – oil, and zirconium oxide. Shell side loop handles hot oil. Shell side loop consist of storage vessel of 40 L capacity with heater of 4.5 kW, control valve, pump and thermostat.

To measure the wall temperature of the tube side and the bulk mean temperature of the fluids at the inlet and out let of the heat exchanger eight thermocouples (T – types) are soldered at places along the test section and four thermocouple (T – types) are inserted at the inlet and out let of the test section. The pressure drop is measured by two gauge pressure. To preserve a constant temperature at the inlet of the test section the heated fluid returns to reservoir tank passing through cooling unit to a cooler fluid. The first test section depicts in figure (2). The second experimental set up consist of pump, heat exchanger with fins (test section), reservoir tank, flow meter (Dwyer series MMA mini – master flow meter) having range of (0.5 – 5.5Lpm), control valve, internal tube, pressure gauges, electrical heater 40L capacity with 2 heaters and thermocouple for temperature measurement. The test section is 1200 mm long, copper internal tube 40 mm diameter, Spiral copper tape around the internal tube 172 mm diameter and Pyrex glass external tube 180 mm diameter. The set – up has helical finned tube side and shell side loop. The shell side loop handles hot oil. The helically finned tube loop handles two types of nanofluids used Ag + oil and ZrO_2 + oil. Four T – type

thermocouples of 0.15 ^{0}C accuracy are used to measure inlet and outlet temperatures of shell and helically finned tube side. Eight (T– type thermocouple were placed at equal interval on the outer surface of helical finned tube to measure the wall temperatures. The thermocouples are placed and glued with epoxy to avoid leakage. The pressure gauges are placed across the helical finned tube to measure the pressure drop with accuracy 2%. The shell is insulated with Acrylic resin coated fiberglass sleeving to minimize the heat loss from shell to the ambient. Oil was tested prior to nanofluid after completion of construction and calibration of the flow loop, testing of the loop's functionality for measuring heat transfer coefficient and viscous pressure loss. The numbers of the total tests were 250. Hot fluid and cold fluid were passed to shell side and helical finned tube side to check the leakages in the circuit and tested the thermocouples and thermostat. The two types of nanofluids at 1%, 2%, 3%, 4%, 5 %, volume concentration was circulated through the helical finned tube side. Hot oil was circulated to the shell side. Helically finned tube side pump is switched on when oil reaching to a prescribed temperature. This done by thermostat attached in oil electrical heater. The flow configuration was made parallel flow condition. The corresponding temperatures were recorded after attaining the steady state. The same procedure was done for nanofluid at 2 % volume concentration. The flow configuration is changed from parallel to counter flow. The same procedure is followed and the temperatures are recorded. Flow rate on helical finned tube (1.5 LPM) and shell are maintained constant throughout the test. The flow rate on helically finned tube side is varied. The flow in tube side is in the range of 0.5 – 3.75 LPM. The second test section has been fabricated as shown in fig.(3) and schematically of the two loops indicated in fig.(4).

Fig .2 The first test section of experimental apparatus

Fig .3 The second test section of experimental apparatus

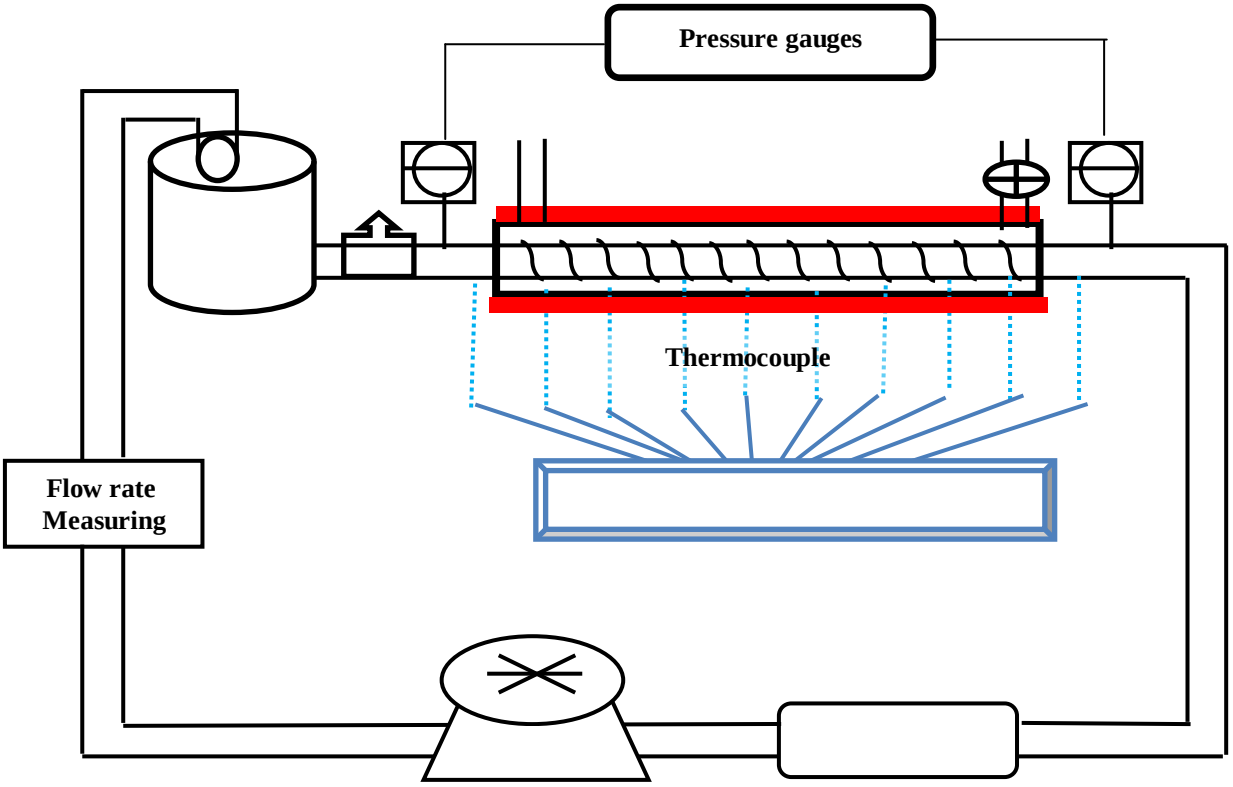

Fig 4. Schematic diagram of experimental apparatus of the convective heat transfer and flow Characteristics for nanofluid

4. Measurement of Nanofluid Thermal Properties

All physical properties of the nanofluids (Ag, ZrO_2 + oil) and oil needed to calculate the pressure drop and the convective heat transfer are measured. The dynamic viscosity (μ) is measured using brook field digital viscometer model DV – E. The thermal conductivity, specific heat and density are measured by Hot Disk Thermal Constants Analyzer (6.1), specific heat apparatus (ESD – 201) as well as the measurement of density was carried out by weighing a sample and volume. The thermal properties of nanofluids dynamic viscosity (μ) , thermal conductivity, specific heat and density are measured with different volume concentrations at 1%, 2%, 3%, 4%, 5 %.

5. Data reduction

The data reduction of the measured results is summarized in the following procedures: Heat transferred from the hot oil in the test section, Q_{oil} can be calculated from

$$Q_{oil} = \dot{m}_{oil} Cp_{oil} \left(T_{out} - T_{in}\right)_{oil} \quad (5)$$

Heat transferred to the nanofluid, Q_{nf} can be calculated from

$$Q_{nf} = \dot{m}_{nf} Cp_{nf} \left(T_{in} - T_{out}\right)_{nf} \quad (6)$$

The average heat transfer rate, Q ave, used in the calculation is determined from the nanofluid side and hot oil side as follows and fouling factor was not taken into account.
:

$$Q_{ave} = \frac{Q_{oil} + Q_{nf}}{2} \quad (7)$$

The shell – side heat transfer coefficient, ho, can be calculated from the average heat transfer rate obtained from

$$Q_{ave} = h_o A_o \left(T_{oil,ave} - T_{nf\,,ave} \right) \quad (8)$$

The overall heat transfer coefficient, Uo, was calculated from the temperature data and the heat transfer rate using the following equation [1984]:

$$U_o = \frac{Q_{ave}}{A_o LMTD} \quad (9)$$

The log mean temperature difference based on the inlet temperature difference,ΔT1, and the outlet temperature difference, ΔT2.

$$LMTD = \frac{\left(\Delta T_2 - \Delta T_1 \right)}{\ln\left(\frac{\Delta T_2}{\Delta T_1} \right)} \quad (10)$$

$$Nu_o = \frac{h_o D_h}{k_{nf}} \quad (11)$$

The hydraulic diameter of shell which is calculated from the following formula:

$$D_h = \frac{4\left(V_{shell} - V_{finned\ tube} \right)}{\pi (D + d)\left(L_{sheel} + L_{finned\ tube} \right)} \quad (12)$$

The outer heat transfer coefficient of shell tube and overall heat transfer coefficient are calculated from Eqs.(8) and (9). The experimental shell tube side Nusselt number is calculated from Eq.(11). An inside heat transfer coefficient, hi, is usually obtained from the overall thermal resistance consisting of three resistances in series: the convective resistance on the outer surface, conductance resistance of the finned tube wall, and the convective resistance on the inner surface. The overall heat transfer coefficient can be related to the inner and outer heat transfer coefficients by the following equation [1984]:

$$\frac{1}{U_o} = \frac{A_o}{A_i h_i} + \frac{A_o \ln\left(\frac{D_i}{d} \right)}{2\pi K L} + \frac{1}{h_o} \quad (13)$$

The Nusslet number in finned tube side is determined by the following definition.

$$Nu_i = \frac{h_i d_i}{k_{nf}} \quad (14)$$

Finally, the following expressions are used to calculate the mean heat transfer coefficient .

$$h(x) = \frac{Nu(x)D}{K} \quad (15)$$

$$\bar{h} = \frac{1}{L}\int_0^L h(x)\,dx \quad (16)$$

$$\Delta p = 32\frac{u_m \mu L}{D_{tube}^2} \quad (17)$$

A new parameter called performance index, η, is defined as follows:

$$\eta = \frac{\left(\frac{h_{mean,\,nf}}{h_{mean\,,\,without\ fins,bf}}\right)}{\left(\frac{\Delta p_{\,nf}}{\Delta p_{without\ fins,\,bf}}\right)} \quad (18)$$

The shear stress can be calculated from

$$\tau = \frac{r\,\Delta p}{2\,L} \quad (19)$$

The strain rate can be calculated from the following formal

$$\gamma = \frac{\tau}{\mu} = \frac{du}{dy} \quad (20)$$

6. Results and Discussion

The uncertainty of experimental results may be originated from the measuring errors of parameters such as temperatures and flow rate. By using the proposed equation of Kline and McClintock [1953], the uncertainty of experimental heat transfer coefficient and Nusselt number was calculated to be about 2 %. The uncertainty of the ratio of nanofluid heat transfer coefficient to that of distilled water, (h_{nf} / h_{Dw}), was about 3.2 %. The uncertainties of experimental data are summarized in Table .4

Table .4 The uncertainty of experimental data

Parameter	h (kW/m^2K)	Nu	h_{nf} / h_w	Δp_{nf} / Δp_w
Uncertainty (%)	**2**	**2**	**3.2**	**0.7**

The reliability and accuracy of the experimental system are estimated by using oil as the working fluid. The heat transfer coefficients are experimentally measured using base oil as the working fluid before obtaining those of oil based Ag and ZrO_2 nanofluids. The experiments are conducted within the Reynolds number of 200. Due to flow low Reynolds number and also, because oil has got high Prandtl number. Experimentally measured Nusselt numbers are

compared against the values obtained by the following theoretical solution presented in [1984].

$$Nu_x = \frac{G_0 \exp\left(-\lambda_0^2 x^+\right)}{2\left(\frac{G_0}{\lambda_0^2}\right)\exp\left(-\lambda_0^2 x^+\right)} \qquad (21)$$

Where: Nu_x is the local Nusselt number, and $X^+ = \frac{2(X/D)}{Re\ Pr}$. λ_n^2 and G_n are defined in Table 5. This solution is used for obtaining local Nusselt number of a nanofluid flow inside straight tube without fins of the heat exchanger under constant wall temperature condition. Having the local heat transfer coefficient at ten axial locations shown in Fig. 3., the average heat transfer coefficient are obtained using Eqs. (15) and (16). Fig. 6 shows the variation of theoretical values with experimental values for average heat transfer coefficient of heat exchanger without fins. As it is seen from this figure, the deviation of the experimental data from the theoretical one is within −4% and +1.5%.

Table 5. The coefficient of λ_n^2 and G_n are used in equation (21)

n	λ_n^2	G_n
0	**7.313**	**0.749**
1	**44.61**	**0.544**
2	**113.9**	**0.463**
3	**215.2**	**0.415**
4	**348.6**	**0.383**

For n > 2, $\lambda_n = 4n + \frac{8}{3}$ and $G_n = 1.01276\ \lambda_n^{-\frac{1}{3}}$.

Also, the measured pressure drop is compared with the pressure drop obtained from the theoretical equation (17).

In which, μ is measured at the average of inlet and outlet temperatures. Fig. 7 shows the variation of the theoretical values for pressure drop along the test section heat exchanger without fins versus measured pressure drop. The experiments are done at the same condition explained in the heat transfer validation. As it can be seen from Fig. 7, the deviation of the experimental data from the theoretical one is within −2% and +3%. Having established confidence in the experimental system, the heat transfer and pressure drop characteristics of oil – based Ag, ZrO_2 nanofluids flowing inside the heat exchanger without and with fins are investigated experimentally for laminar flow conditions. Note that in the following results, heat transfer coefficient and pressure drop data for each two specific cases are not achieved under exactly the same Reynolds numbers. This is because the viscosity of oil based nanofluid is so dependent on fluid temperature and particle volume fraction.

Figs. (8 , 9, 10 and 11). Exhibit the variation of heat transfer coefficient versus Reynolds number for the flow of base oil and the nanofluids (Ag + oil, ZrO_2 + oil) with different nanoparticle volume concentrations inside the heat exchanger without and with fins. The

addition nanoparticle of silver and zirconium oxide to the base oil has led to an increase in mean heat transfer coefficient for flow inside both the heat exchanger without and with fins. In general the addition of nanoparticles enhances the thermal conductivity of the base fluid. This enhancement in thermal conductivity would increase the convective heat transfer coefficient. As well as, chaotic movement of the nanoparticles in flow will disturb the thermal boundary layer formation on the internal tube surface wall of heat exchanger. As a result of this disturbance, the development of the thermal boundary layer is delayed. Since, higher heat transfer coefficient of nanofluid flow in a heat exchanger are obtained at the thermal entrance region, the delay in thermal boundary layer formation resulted by adding nanoparticles will increase the heat transfer coefficient. At higher volume concentrations of the nanofluids, both the thermal conductivity of the Ag, ZrO_2 + base oil mixture and the disturbance effect of the nanoparticles will increase. Therefore, as it is expected, nanofluids with higher volume concentrations have generally higher mean heat transfer coefficient.

Figs. (12 and 13) reveal the ratios of mean heat transfer coefficient of nanofluids with 5 % volume fractions to that of base oil as a function of Reynolds number for the heat exchanger without and with fins. It is observed that nanofluids (Ag + oil, ZrO_2 + oil) have better heat transfer performance when they flow inside heat exchanger with fins instead of flowing inside the heat exchanger without fins. The results clearly show that at nearly the same range of Reynolds numbers, the highest heat transfer coefficient ratios are obtained for the heat exchanger with fins. For instance, a maximum increase of 22.41 % (Ag+ Oil) and 16.25 % (ZrO_2+ Oil) in heat transfer coefficient ratio for a range of Reynolds numbers between 20 and 200 is obtained for the heat exchanger without fins , while, the increase of 38.5% (Ag+ Oil) and 25.33 % (ZrO_2+ Oil) is obtained for the heat exchanger with fins, respectively at the same Reynolds numbers' range. This phenomenon could be due to the intensified chaotic motion of the nanoparticles inside heat exchanger with fins. Since, the shear rate near the internal tube wall of the heat exchanger with fins is high, the non-uniformity of the shear rate across the cross section will increase and therefore, the particles are more motivated by the variation of the shear rate. The latter point suggests that applying nanofluids instead of the base fluid would enhance the convective heat transfer more effectively in the heat exchanger with fins.

Figs.(14 and 15) depicted the variation of mean heat transfer coefficient versus Reynolds number for the heat exchanger without and with fins. This comparison is made for base oil and 5 % vol nanofluids (Ag + oil , ZrO_2 + oil) flow at constant wall temperature, in order to have a close examination in the behavior of heat exchanger with fins. Obtained results show that heat exchanger with fins has increased heat transfer rates significantly compared to those of heat exchanger without fins. The possible mechanisms which are responsible for heat transfer enhancement in heat exchanger with fins could be attributed to the change in temperature and velocity distributions along the heat exchanger with fins cross section. As fluid flows within heat exchanger with fins, it experiences a centrifugal is generated. A secondary flow induced by the centrifugal force has significant ability to enhance the heat transfer rate by increasing the velocity gradient across the section of the heat exchanger. As a result, heat is transferred more rapidly in the heat exchanger with fins.

The measured pressure drop for the flow of base oil and Ag, ZrO_2 + base oil nanofluids with different volume fractions as a function of Reynolds number along the heat exchanger

without and with fins is given in Figs. (16, 17, 18 and 19), respectively. The results exhibit that there is a noticeable increase in pressure drop of nanofluid with 1% vol nanoparticle concentration compared to the oil value. This enhancement trend tends to continue for the nanofluids with higher volume fractions. This is because of the fact that suspending solid particles in a fluid generally increases dynamic viscosity relative to the base fluid. Since, the viscosity is in direct relation with pressure drop, the higher value of viscosity leads to increased amount of pressure drop. Another reason which can be responsible for pressure drop increasing of nanofluids may be attributed to the chaotic motion and migration of nanoparticles in the base fluid. This reason explains why at higher flow rates, the rate of increase in pressure drop has gone up while at very low Reynolds numbers, the pressure drops of base oil and nanofluids are almost the same. However, the rate of pressure drop increasing achieved for nanofluids with concentration ranges from 1% vol to 5% vol is less than that obtained when nanofluid with 1 % vol fraction is used instead of oil. One reason for this behavior may be due to the anti – friction properties of Ag, ZrO_2 nanoparticles. Ag, ZrO_2 nanoparticles are basically spherical.

The spherical shape of nanoparticles may result in rolling effect between the rubbing surfaces and the situation of friction is changed from sliding to rolling, thus the lubricant with nanoparticles achieves a good friction reduction performance. The rolling effect of nanoparticles was also reported by Battez et al. [2008] and Wu et al. [2007]. As well as it is concluded that for heat exchanger without fins, the maximum pressure drop increasing of about 14.3% (Ag + oil) and 10.1% (ZrO_2+oil) are achieved when nanofluid with 5 % vol concentration is used instead of base fluid. However, for the heat exchanger with fins, the maximum pressure drop enhancement of 20.41 % (Ag + oil) and 15.2 % (ZrO_2+oil) are obtained. It means that, the rate of pressure drop increasing due to the using of nanofluid is more prominent in the heat exchanger with fins. When applying heat exchanger with fins instead of the heat exchanger without fins and using nanofluid flow inside the test sections instead of the base liquid flow, enhanced the convective heat transfer coefficient. However, these enhanced heat transfer techniques were both accompanied with increase in pressure drop which can limit the use of them in practical applications. Therefore, in order to find the optimum work conditions, a further study on the overall performance of these techniques should be carried out to consider pressure drop enhancement besides heat transfer augmentation, simultaneously.

Apparently, when the performance index is greater than 1, it implies that the heat transfer technique is more in the favor of heat transfer enhancement rather than in the favor of pressure drop increasing. Therefore, the heat transfer methods with performance indexes greater than 1 would be feasible choices in practical applications. Figs. (20, 21, 22 and 23) reveal the variation of performance index versus Reynolds number for nanofluids (Ag + oil) and (ZrO_2 + oil) with different volume concentrations flowing inside the heat exchanger without and with fins at constant wall temperature. Here, h_{nf} and ΔP_{nf} in Eq. (18) are the mean heat transfer coefficient and pressure drop of the nanofluid flow inside the heat exchanger without fins, respectively.

Figs (20,and 21) it is seen that the performance index is greater than 1 just for nanofluids with 1 ,3 ,and 5% vol concentrations. The maximum performance index of 1.1 and 1.02 are obtained for the nanofluids (Ag + oil) and (ZrO_2 + oil) with 5%vol concentration at Reynolds

number of 190 and the heat exchanger without fins. While figures (22,and 23) in the heat exchanger with fins 1.5 and 1.32 respectively for the same nanofluids. Also It is seen from these figures that the, all concentration for the heat exchanger with fins has performance indexes greater than 1. It means that for base flow along the heat exchanger with fins, the rate of increasing in pressure drop is lower than increasing in heat transfer coefficient. In addition, it is evident from Figs. (20, 21, 22 and 23) that applying heat exchanger with fins instead of the heat exchanger without fins is a more effective way to enhance the convective heat transfer compared to using nanofluids instead of the base fluid. This relatively high performance index suggests that applying both of the heat transfer enhancement techniques studied in this investigation is a good choice in practical application.

Figs.(24 – 29) shows the flow curve shear stress is plotted against shear rate for nanofluids (Ag + oil) and (ZrO_2 + oil) at 1%, 2%, 3%, 4% and 5% particle volume concentration. The plot data for these types of nanofluid are not parallel, indicating that the materials are a Newtonian fluid over this range of shear stress. As well as these figures indicated the shear stress increases with an increasing shear rate, for nanofluids. These figures indicated the flow curve of the nanofluids measured using the heat exchanger without and with fins. The shear stress of nanofluids increases with an increase in concentration of nanoparticles for both parallel flow and counter flow. The use of nanofluid significant gives higher heat transfer coefficient than oil as based fluid. Nanofluids that contain metal nanoparticles silver (Ag) show more enhancements compared to oxide zirconium(ZrO_2) nanofluids. Figs.(30 – 33) shows no much impact of changing flow direction on overall heat transfer coefficient and the nanofluids behaves as the Newtonian fluid for ranging from (1% – 5%) .

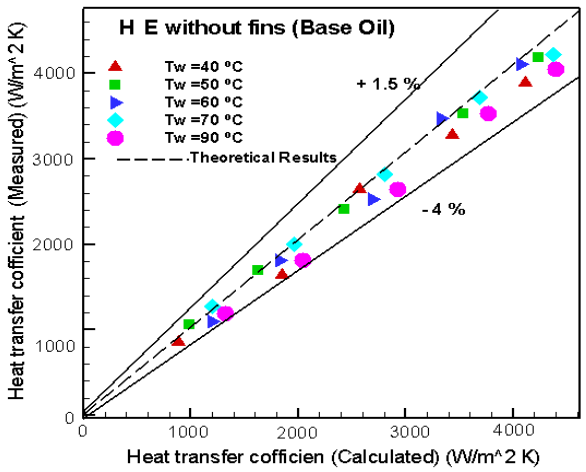

Fig 6. Comparison between theoretical and experimental heat transfer coefficient of base oil

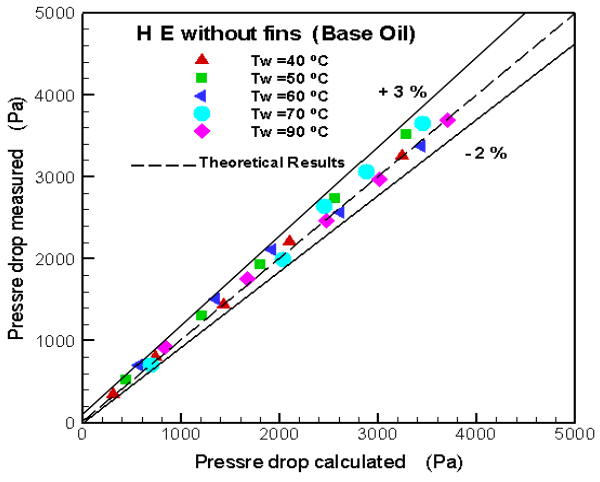

Fig 7. Comparison between theoretical and experimental pressure drop of base oil

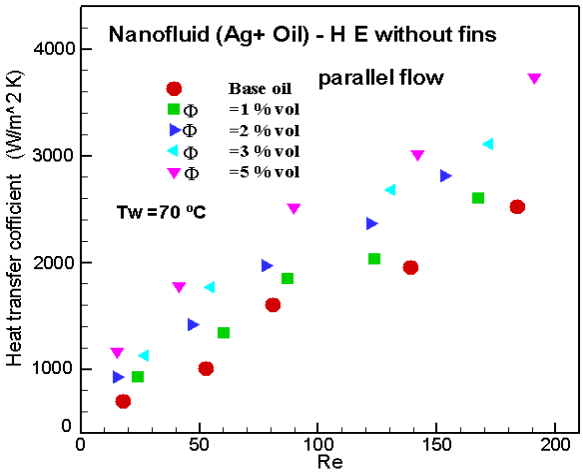

Fig 8. Variation of heat transfer coefficient with Re to nanofluid (Ag +oil) in HE without fins

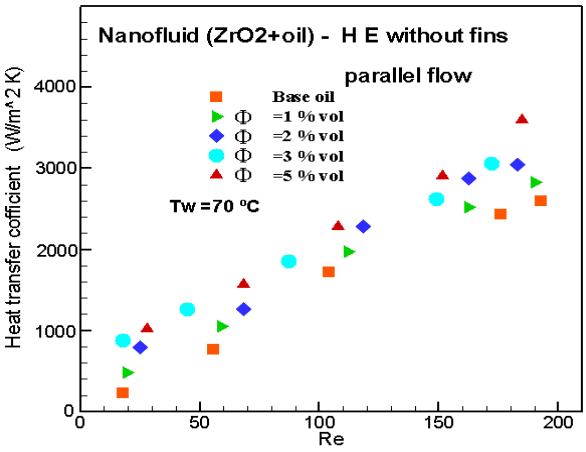

Fig 9. Variation of heat transfer coefficient with Re to nanofluid (ZrO_2+oil) in HE without fins

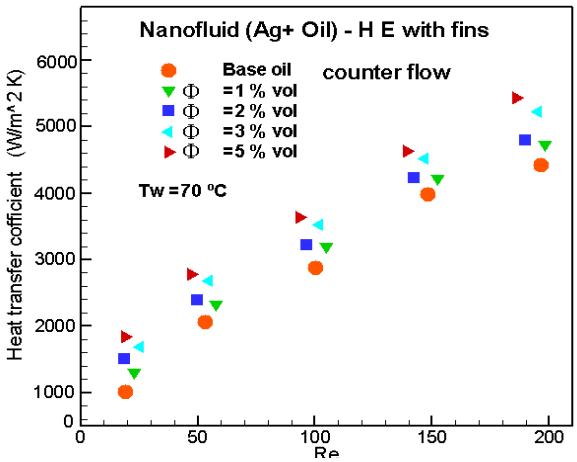

Fig 10. Variation of heat transfer coefficient with Re to nanofluid (Ag +oil) in HE with fins

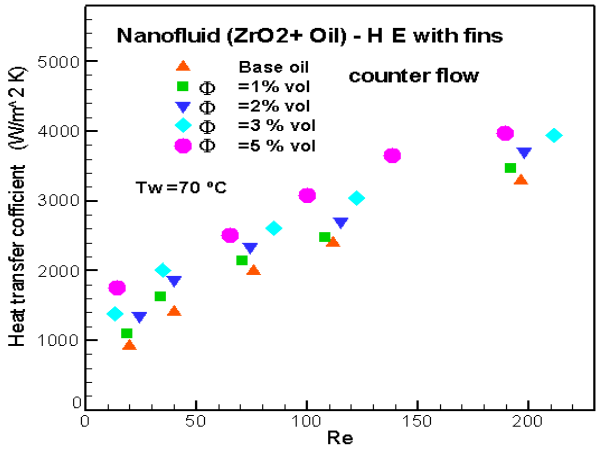

Fig 11. Variation of heat transfer coefficient with Re to nanofluid (ZrO_2+oil) in HE with fins

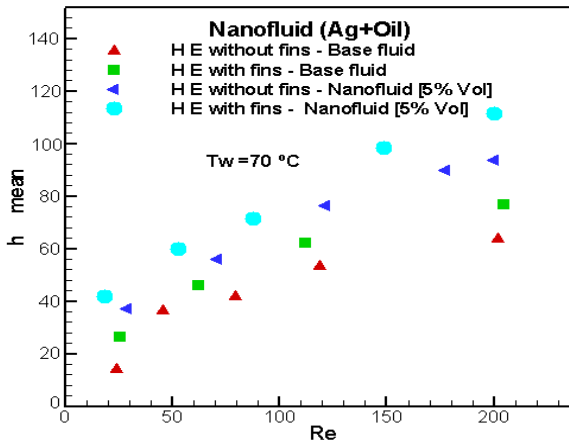

Fig 12. Variation of h versus Re to nanofluid (Ag + oil) in HE with and without fins

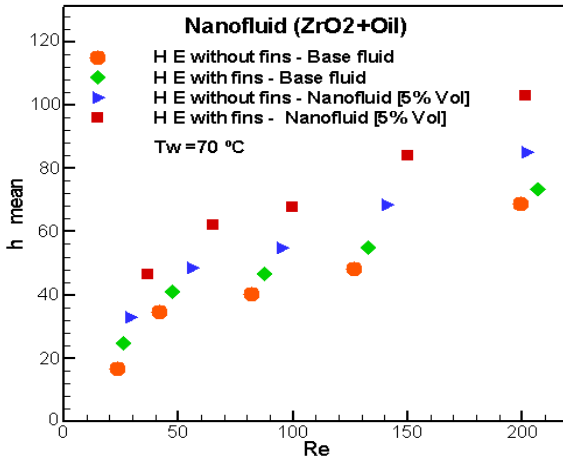

Fig 13. Variation of h versus Re to nanofluid (ZrO_2 + oil) in HE with and without fins

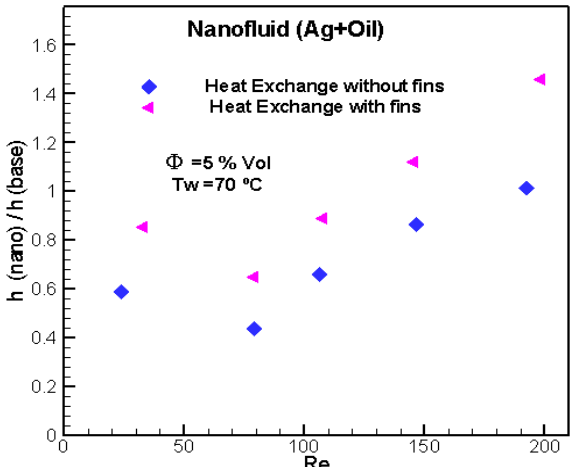

Fig 14. The h ratio versus Re to nanofluid (Ag + oil) in HE with and without fins at CWT

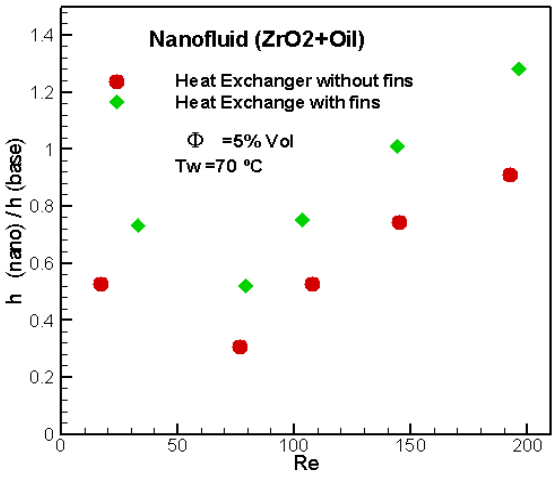

Fig 15. The h ratio versus Re to nanofluid (ZrO_2 + oil) in HE with and without fins at CWT

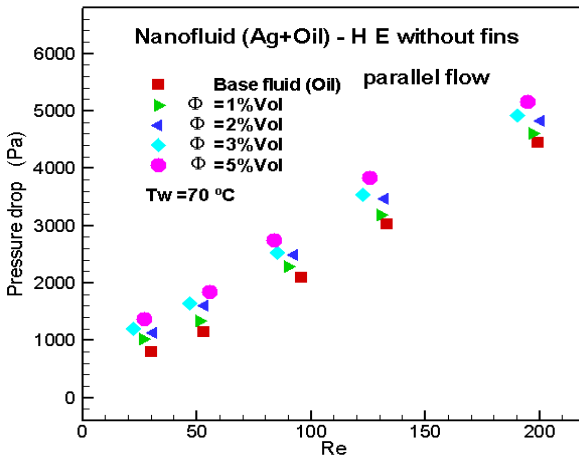

Fig 16. Pressure drop versus Re to nanofluid(Ag + oil) in HE without fins

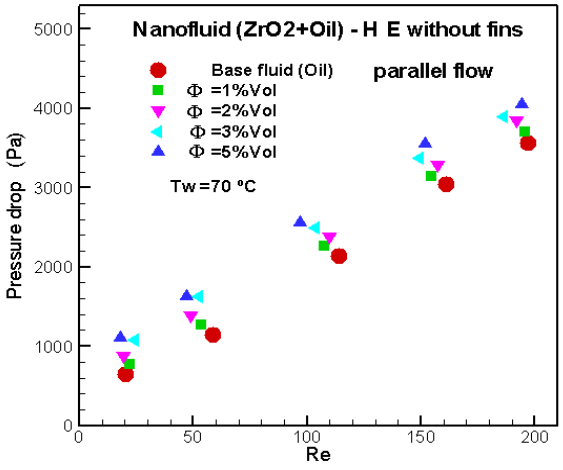

Fig 17. Pressure drop versus Re to nanofluid(ZrO_2 + oil) in HE without fins

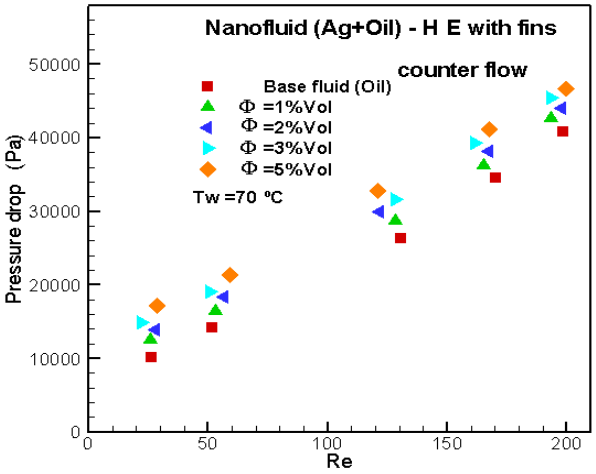

Fig 18. Pressure drop versus Re to nanofluid(Ag + oil) in HE without fins

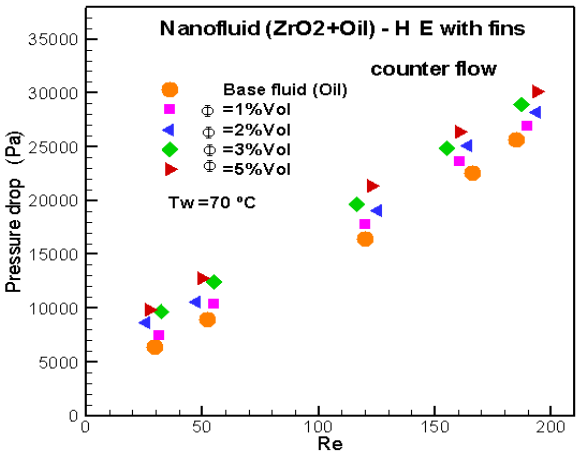

Fig 19. Pressure drop versus Re to nanofluid(ZrO_2 + oil) in HE without fins

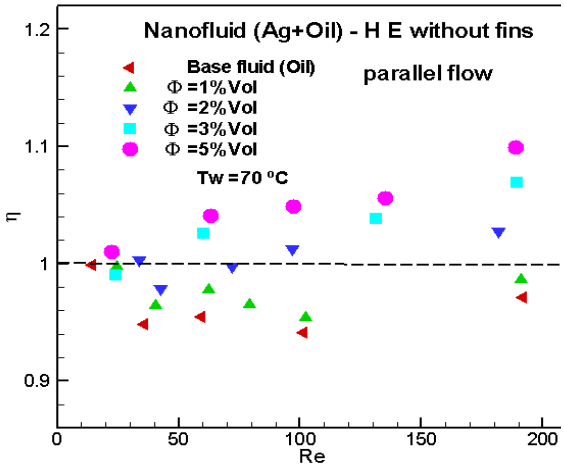

Fig 20. The performance index versus Re to nanofluid (Ag + oil) in HE without fins

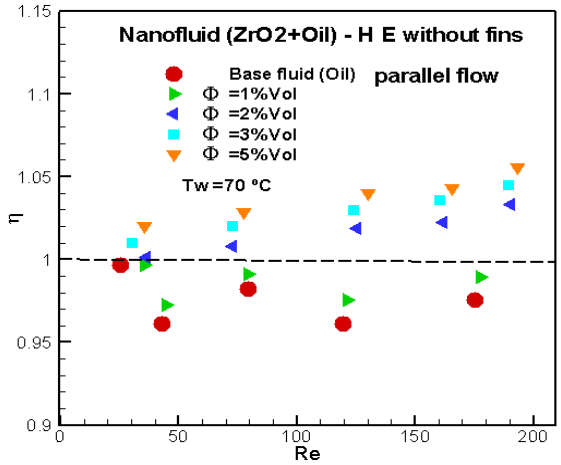

Fig 21. The performance index versus Re to nanofluid (ZrO_2 + oil) HE without fins

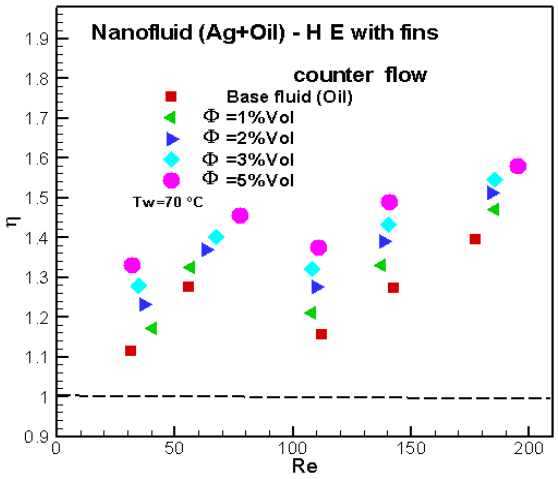

Fig 22. The performance index versus Re to nanofluid(Ag + oil) in HE with fins

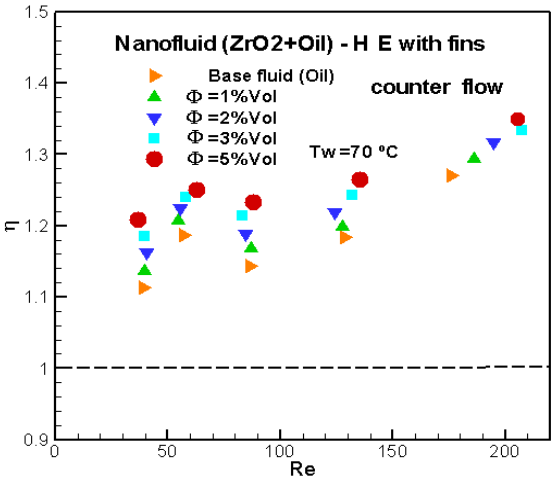

Fig 23. The performance index versus Re to nanofluid (ZrO_2 + oil) HE with fins

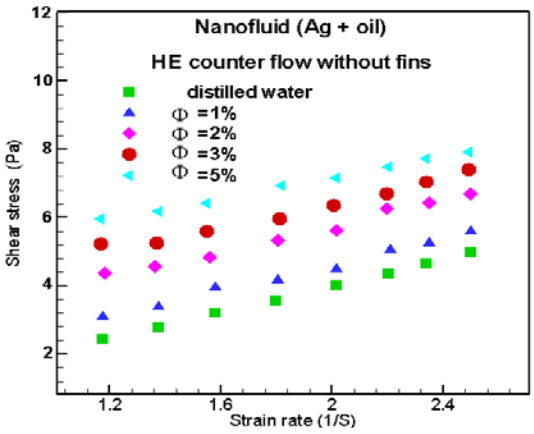

Fig.24 Shear stress versus shear rate for nanofluid (Ag + oil) counter flow without fins

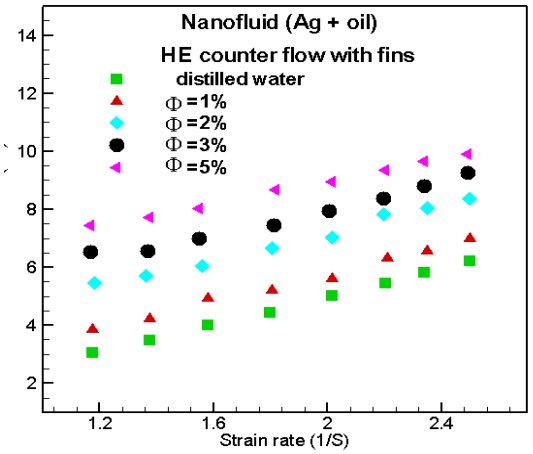

Fig.25 Shear stress versus shear rate for nanofluid (Ag + oil) counter flow with fins

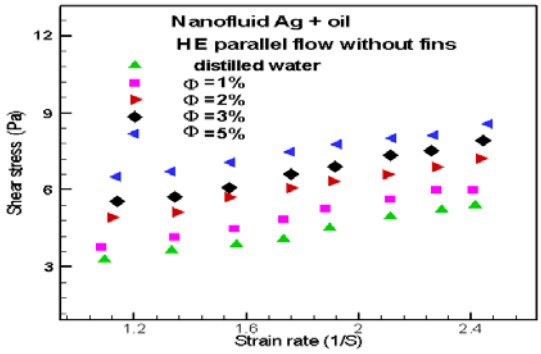

Fig.26 Shear stress versus shear rate for nanofluid (Ag + oil) parallel flow without fins

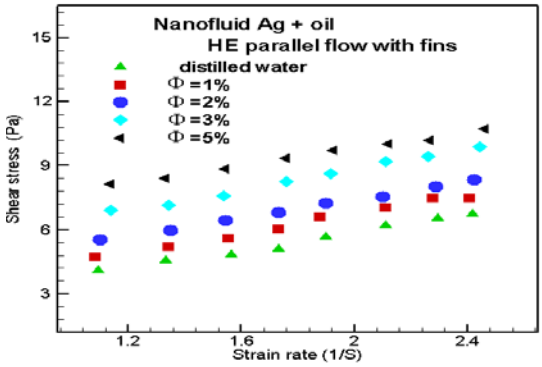

Fig.27 Shear stress versus shear rate for nanofluid(Ag + oil) parallel flow with fins

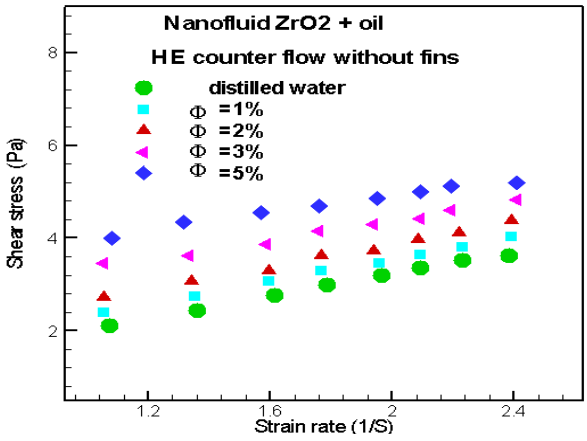

Fig. 29 Shear stress versus shear rate for nanofluid (ZrO_2 + oil) counter flow without fins

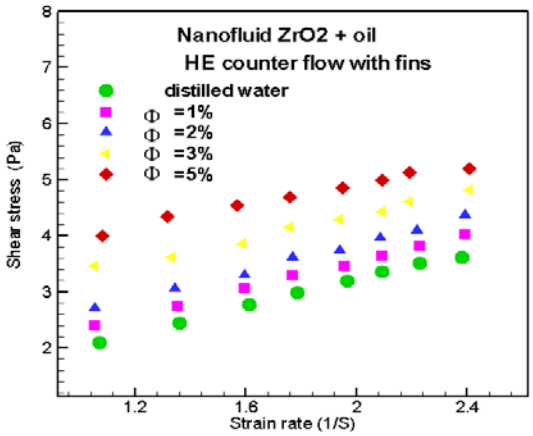

nanofluid (ZrO_2 + oil) counter flow with fins

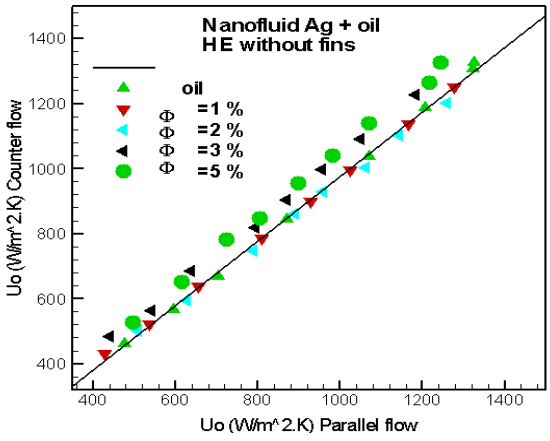

Fig.30 Compression of overall heat transfer coefficient of parallel and counter flow configuration for nanofluid (Ag + oil) HE without fins

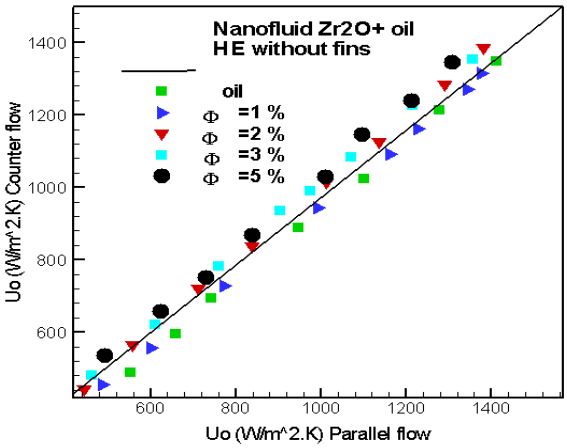

Fig.31 Compression of overall heat transfer coefficient of parallel and counter flow configuration for nanofluid(ZrO_2 + oil) HE without fins

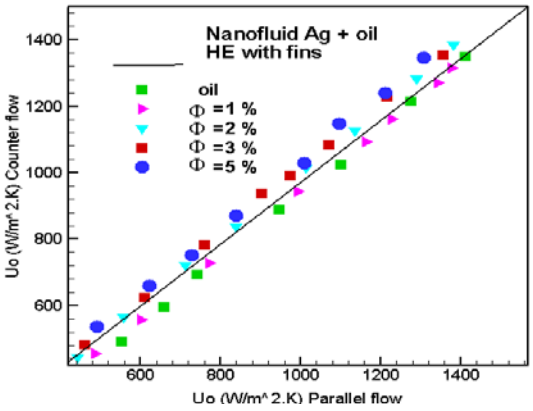

Fig.32 Compression of overall heat transfer coefficient of parallel and counter flow configuration for nanofluid(Ag + oil) HE with fins

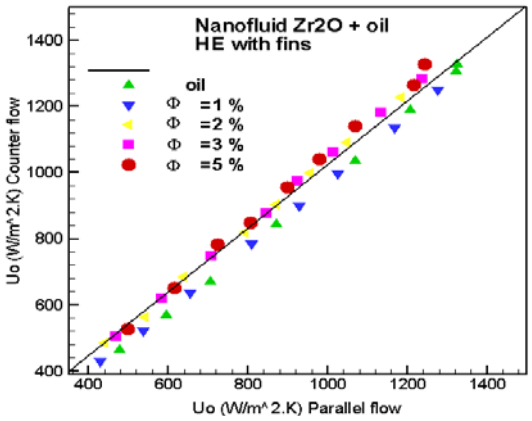

Fig.33 Compression of overall heat transfer coefficient of parallel and counter flow configuration for nanofluid(ZrO_2 + oil) HE with fins

7. Conclusion

The following conclusions are drawn from this study:

1. The nanoparticles type and volume concentration in nanofluid plays an important role in enhancement of heat transfer rate
2. The heat exchanger with fins enhances the heat transfer rates compared to that of the heat exchanger without fins, significantly at constant nanoparticle concentration and using nanofluids.
3. Nanofluids have better heat transfer characteristics when they flow in heat exchanger with fins rather than in the heat exchanger without fins. Compared to base oil flow.
4. Metal nanofluid (Ag + oil) have better mean heat transfer coefficient and pressure drop in heat exchanger with fins rather than oxide nanofluid (ZrO_2+ oil) in the heat exchanger without fins. Compared to base oil flow.
5. The performance index for the nanofluid flow inside the heat exchanger with fins is greater than the performance index for the nanofluid flow inside the heat exchanger without fins comparing with the base oil flow. This relatively high performance index suggests that applying both of the heat transfer enhancement techniques studied in this investigation is a good choice in practical application.
6. The pressure drop of nanofluids in heat exchanger with fins is greater than pressure drop of nanofluids in the heat exchanger without fins as well as compared to that of base liquid.
7. The shear stress of nanofluids increases with an increase in concentration of nanoparticles for both parallel flow and counter flow in heat exchanger.
8. No much impact of changing flow direction on overall heat transfer coefficient and the nanofluids (Ag, and ZrO_2 + oil) behaves as the Newtonian fluid for ranging from (1% – 5%) .

8. References

1. **A.E.** Bergles, Recent development in convective heat transfer augmentation, Applied Mechanics Reviews 26 (1973) 675–682.
2. A.H. Battez, R.G. alez, J.L. Viesca, J.E. Fernandez, J.M. Diaz Fernandez, A. Machado,R. Chou, J. Riba, CuO, ZrO2 and ZnO nanoparticles as anti – wear additive in oil lubricants, Wear 265 (2008) 422–428.
3. B. Pak, Y.I. Cho, Hydrodynamic and heat transfer study of dispersed fluids with submicron metallic oxide particle, Experimental Heat Transfer 11 (1998)151–170.
4. Choi, and colleagues, Preparation and heat transfer properties of nanoparticle- in-transformer oil dispersions as advanced energy-efficient coolants. Current Applied Physics, 2008. 8(6): p. 710-712.
5. D.G. Prabhanjan, G.S.V. Raghavan, T.J. Rennie, Comparison of heat transfer rates between a straight tube heat exchanger and a helically coiled heat exchanger, International Communication of Heat Mass Transfer 29 (2002) 185–191.
6. D. Wen, Y. Ding, Experimental investigation into convective heat transfer of nanofluids at the entrance region under laminar flow conditions, International Journal of Heat and Mass Transfer 47 (2004) 5181–5188.
7. F.M. White, Heat Transfer, Addison – Wesley Publishing CompanyInc., New York, NY, (1984).
8. H.A. Mintsa, G. Roy, C.T. Nguyen, D. Doucet, New temperature dependent thermal conductivity data for water-based nanofluids, International Journal of Thermal Sciences 48 (2009) 363–371.
9. J.R. Thome, Engineering Data Book III, Wolverine Tube Inc, 2006.

Kline, S.J., McClintock, F.A., Describing uncertainties in single – sample experiments. Mechanical Engineering 75 (1), 3 – 8,(1953).

10. M. Chandrasekar, S. Suresh, A. Chandra Bose, Experimental investigations and theoretical determination of thermal conductivity and viscosity of Al_2O_3/water nanofluid, Experimental Thermal and Fluid Science 34 (2010) 210–216.
11. M. Chandrasekar, S. Suresh, A. Chandra Bose, Experimental studies on heat transfer and friction factor characteristics of Al2O3/water nanofluid in a circular pipe under laminar flow with wire coil Inserts, Journal of Thermal and Fluid Science 34 (2010) 122–130.
12. N.R. Karthikeyan, J. Philip, B. Raj, Effect of clustering on the thermal conductivity of nanofluids, Materials Chemistry and Physics 109 (2008) 50–55.
13. R.S. Vajjha, D.K. Das, Experimental determination of thermal conductivity of three nanofluids and development of new correlations, International Journal of Heat and Mass Transfer 52 (2009) 4675– 4682.
14. R.C. Xin, A. Awwad, Z.F. Dong, M.A. Ebadian, An experimental study of single phase and two-phase flow pressure drop in annular helicoidally pipes, International Journal of Heat Fluid Flow 18 (1997) 482–488.
15. S.U.S. Choi, Enhancing thermal conductivity of fluids with nanoparticles, ASME FED 231 (1995) 99–105.

16. S.M. Fotukian, M. Nasr Esfahany, Experimental study of turbulent convective heat transfer and pressure drop of dilute CuO/water nanofluid inside a circular tube, International Communications in Heat and Mass Transfer 37 (2010) 214–219.
17. W. Yu, H. Xie, L. Chen, Y. Li, Enhancement of thermal conductivity of kerosene based Fe_3O_4 nanofluids prepared via phase-transfer method, Colloids and Surfaces A: Physicochemical and Engineering Aspects 355 (2010) 109–113.
18. US Research Nanomaterials, Inc. 3302 Twig Leaf Lane, Houston, TX 77084, USA Phone: (Sales) 832 – 460 – 3661 ; (Shipping) 832 – 359 – 7887 Fax: 281 – 492 – 8628,2014 ,Service@us-nano.com ; Tech@us-nano.com
19. W.C. Williams, J. Buongiorno, L.W. Hu, Experimental investigation of turbulent convective heat transfer and pressure drop of alumina/water and zirconia/ water nanoparticle colloids (nanofluids) in horizontal tubes, Journal of Heat Transfer 130 (2008) 2412–2419.
20. Website, http://WWW.CASTROL.COM/US , Castrol (GTX) Company, BP Lubricants USA Oil Company, 46, USA,2014.
21. Y. He, Y. Jin, H. Chen, Y. Ding, D. Cang, H. Lu, Heat transfer and flow behavior of aqueous suspensions of TiO2 nanoparticles (nanofluids) flowing upward through a vertical pipe, International Journal of Heat Mass Transfer 50 (2007) 2272–2281.
22. Y. Ding, H. Alias, D. Wen, A.R. Williams, Heat transfer of aqueous suspensions of carbon nanotubes, International Journal of Heat and Mass Transfer 49 (2006)240–250.
23. Y. Xuan, Q. Li, Investigation on convective heat transfer and flow features of nanofluids, Journal of Heat Transfer 125 (2003) 151–155.
24. Y.Y. Wu, W.C. Tsui, T.C. Liu, Experimental analysis of tribological properties of lubricating oils with nanoparticle additives, Wear 262 (2007) 819–825.

9. Nomenclature

Re	Reynolds number	—
Pr	prandl number	—
ΔP	Pressure drop	pa
HE	Heat exchanger	—
k_n	Thermal conductivity of nanofluid	$W/m^2.K$
$\dot{m}_{oil}$	The mass flow rate of hot oil	kg/s
Cp_{oil}	The specific heat of oil	Kj/kg
Toil, in and Toil, out	The inlet and outlet hot oil temperatures	^0C
Toil, ave	The average oil temperature,	^0C
Tnf, ave	The average nanofluid temperature	^0C
Ao	The outside surface area of tube	m^2

Q_{ave}	The heat transfer rate	kJ
D_h	The hydraulic diameter of shell	m
LMTD	The log mean temperature difference	—
$\Delta T1$	The inlet temperature difference	^0C
$\Delta T2$	The outlet temperature difference	^0C
Di	The inner diameter of the shell	m
d	The diameter of the inner finned tube	m
K	The thermal conductivity of the tube	W/ m K
L	The length of the heat exchanger.	m
h_{mean}	Mean heat transfer coefficient	kJ/m^2 k
	Creek letters	
μ_n	Dynamic viscosity of nanofluid	$N.s/m^2$
ρ_n	Density of nanofluid	kg/m^3
η	Index performance	—
Φ	Nanoparticle volume fraction	—
γ	Shear rate	s^{-1}
τ	Shear stress	Pa
	subscripts	
n	Nanofluid	—
b	Base fluid	—
i	Inner	—
o	outer	—
bf	Base fluid (oil)	bf